北里大学大学院理学研究科

平成２８年度博士論文

Masculinization-related genes and cell-mass structures during early gonadal differentiation in the African clawed frog *Xenopus laevis*

和田 美加子（DS-14902）

指導教授　遺伝子機能発現学　高松 信彦

CONTENTS

ABSTRACT

The African clawed frog *Xenopus laevis* has a female heterogametic ZZ/ZW-type sex-determining system. Previously my laboratory members discovered a W-linked female sex-determining gene *dm-W* that was involved in ovary formation probably through the up-regulation of the estrogen synthesis gene *cyp19a1*. They also reported that a unique "mass-in-line structure", which disappears from ZZ gonads during early testicular development, could serve as the base for ovary differentiation in ZW gonads. However, the molecular mechanisms underlying early masculinization including deconstruction of the mass-in-line structure are poorly understood. To elucidate the development of bipotential gonads into testes after sex determination in this species, I focused on the orthologs of five mammalian sex-related genes: three nuclear factor genes, *dax1*, *sf1* (also known as *ad4bp*), and *sox9,* and two genes encoding members of the tumor growth factor-β (TGF-β) family, *anti-Müllerian hormone* (*amh*) and *inhibin βb* (*inhbb*). Quantitative RT-PCR analysis revealed that the expression of *dax1, sox9, amh*, and *inhbb* or *sf1* was greatly or slightly higher in ZZ than in ZW gonads during early sex development. In situ hybridization analysis revealed that *amh* and *inhbb* mRNAs were expressed in somatic cells on the inner and outer sides of cell masses in the mass-in-line structure, respectively, in the developing ZZ gonads. Because a homodimer of INHBB is called Activin B, I built up a hypothesis that it could function as a deconstruction factor for the mass-in-line structure during construction of primary testicular structure. Then I examined an effect of estrogen,

indicating that it also repressed the collapse of the mass-in-line structure in developing ZZ gonads. These findings suggest that TGF-β signaling is involved in the deconstruction of the mass-in-line structure, which could be maintained by estrogen.

INTRODUCTION

Genetic sex-determining systems in vertebrates include female heterogametic ZZ/ZW- and male heterogametic XX/XY-types. Sex-determining genes on the sex chromosomes specify gonadal sex, leading to primary ovarian or testicular formation. My laboratory members previously reported a W-linked gene *dm-W* as a female sex-determining gene in the African clawed frog *Xenopus laevis*, which has a ZZ/ZW-type system (Yoshimoto et al., 2008; Yoshimoto and Ito, 2011). In addition, Okada et al. (2009) revealed that DM-W as a transcription factor might indirectly induce female-specific expression of *cyp19a1*, which encodes estrogen-synthesizing enzyme aromatase and a transcription factor gene *foxl2* in early ovary formation. In fact, immediately after sex determination, *cyp19a1* is predominantly expressed in ZW gonads, whereas the expression of the steroid 17α-hydroxylase gene *cyp17a1* was substantially higher in ZZ gonads than in ZW (Mawaribuchi et al., 2014). They also reported that the mRNA levels of *dmrt1*, which is a prototype gene of *dm-W*, showed no significant difference between ZW and ZZ gonads during tadpole development on quantitative RT-RCR analysis. However, we recently reported that its protein displays dimorphic localization in developing and adult gonads; DMRT1 is expressed in ZZ somatic cells throughout development after sex determination, but not in ZW somatic cells, and also shows its localization in both ZZ and ZW germ stem cells during tadpole development (Fujitani et al., 2016). Moreover, Mawaribuchi et al. (2014) discovered a unique mass-in-line structure with several masses of cells each surrounded by a

basement membrane, aligned along the anteroposterior axis in early differentiating gonads after sex determination; *cyp19a1* or *cyp17a1*/*cyp19a1* are expressed in the cell masses in the ZW or ZZ gonads, respectively. During early ovary development in ZW gonads, ovarian cavities are formed inside cell masses. Interestingly, the mass-in-line structure disappears during testicular development in ZZ gonads. In other words, the mass-in-line structure might be formed in advance to produce ovarian cavities in both ZW and ZZ gonads just after sex determination. However, the construction of ovarian cavities from cell masses in ZW gonads and the loss of mass-in-line structure in ZZ gonads remain unknown.

In the present study, I investigated expression patterns of *X. laevis* orthologs for several mammalian sex-related genes during gonadal development to understand molecular mechanisms of early testicular differentiation in *X. laevis*. A higher expression of the dosage-sensitive sex reversal, adrenal hypoplasia critical region, on chromosome X, gene 1 (*dax1*) and *sry-type HMG box9* (*sox9*) was observed in ZZ than in ZW gonads. In addition, I observed that the expression of two genes encoding members of the tumor growth factor (TGF)-*β* family, anti-Müllarian hormone (*amh*) and inhibin *β*b (*inhbb*), was substantially higher in ZZ than in ZW gonads throughout gonadal development immediately after sex determination and were distinctly localized in cell masses of ZZ gonads at stage 53 after sex determination. Finally, I discuss how the mass-in-line structure is maintained and destructed during early sexual differentiation of gonads after sex determination.

MATERIALS AND METHODS

Animal care and use

All of the experimental procedures involving *X. laevis* were approved by the Institutional Animal Care and Use Committee of Kitasato University. *X. laevis* frogs at various developmental stages were purchased from Watanabe Zoushoku (Yachiomachi, Japan) and maintained at 22°C.

Determining ZW or ZZ Status in *X. laevis*

The ZZ or ZW status of the gonads was determined by genomic PCR as described previously (Yoshimoto et al., 2008).

Real-time reverse transcription PCR (RT-PCR)

Total RNAs were isolated from ZZ and ZW gonads at various stages of development, using the RNeasy Mini Kit (Qiagen, Venlo, Netherlands). RNA was reverse transcribed with the Transcriptor First Strand cDNA Synthesis Kit (Roche, Basel, Switzerland), according to the manufacturer's instructions. Real-time RT-PCR was carried out using a specific primer pair as follows: 5'-TACCCACATAAACTCAGCTACAG-3' and 5'-GTGATCGFTTGGGGTCAAG-3' for *amh.S*, 5'-CTGCATCATCCTTTCACACG-3' and 5'-CCACAATCAT GTTGGGTACG-3' for *inhbb.L,* 5'-CCAATGAGGGGAACCAGAAC-3' and 5'-GCATCCTGGAAATGCACC-3' for *inhbb.S*, 5'-GCTTGCTTAGATAAATGTCA-3'

and 5’-GCCTCAGCAGTGCTGGTG-3’ for *dax1*, 5’-ACTACTCCTCCTTCCAAAGC-3’ and 5’-CGGAATATCTGGTGGAGAGC-3’ for *sf1*, and 5’-CAAAGGACACACATCAAGAC-3’ and 5’-GTATGAAGAGCTGTAATGCTG-3’ for *sox9*. Their expression levels were normalized to the level of *ef-1a*, which was amplified using a specific primer pair, 5’-CCAGATTGGTGCTGGATATG-3’ and 5’-TTCTGAGCAGACTTTGTGAC-3’. Sequence information of the cDNAs was obtained form the following accession numbers: XM_018243639 (*amh.S*), NM_001090586 (*inhbb.L*), XM_018238661 (*inhbb.S*), XM_018246171 (*dax1.L*), XM_018248695 (*dax1.S*), NM_001097969 (*sf1.L*), NM_001094473 (*sox9.L*), NM_001090807 (*sox9.S*), and NM_001087442 (*ef-1a*). The SYBR Green I from the SYBR Green Realtime PCR Master Mix (Toyobo, Osaka, Japan) was used as the fluorescent reporter.

Whole mount in situ hybridization (WISH)

Gonads along with mesonephros at various stages were fixed with a solution of 10% formaldehyde, 0.1 M 3-[N-morpholino]propanesulfonic acid-NaOH (pH 7.4), 4 mM EGTA, and 1 mM $MgSO_4$ for 2 hours. The fixed samples were permeabilized by proteinase K (20 μg/mL) in 0.7×PBS containing 0.1% Tween 20 for 15 min at 37°C, placed in 0.25% acetic anhydride in 0.1 M triethanolamine (pH 8.0), and then refixed with 3.7% paraformaldehyde in 0.1 M TEA for 1 hour at room temperature. They were then hybridized in hybridization buffer (50% formamide, 5×saline sodium citrate, 10 mM dithiothreitol, 1 μg/μL torula yeast RNA, 100 μg/mL heparin, 0.1% Tween 20)

containing 1.5 μg/ml of heat-denatured digoxigenin (DIG)-labeled riboprobes overnight at 52°C for *inhbb.S* and at 60°C for *amh.S*. After hybridization, the samples were washed with buffer (50% formamide, 5x saline sodium citrate). The color reaction was performed as described previously (Mawaribuchi et al., 2014).

The antisense and sense riboprobes corresponding to the coding sequence of *amh.S* (416-935) nucleotides downstream of the A in the translation initiation codon AUG (XM_018243639) or *inhbb.S* (55-815) nucleotides downstream of the A in the translation initiation codon AUG (XM_018238661), which was cloned into pSTP18 (Roche, Basel, Switzerland), were synthesized by T7 RNA polymerase using the DIG RNA labeling kit (Roche, Basel, Switzerland).

Immunohistochemistry

After WISH analysis, the samples were fixed in Bouin's solution (15:5:1 saturated aqueous picric acid solution-formalin-acetic acid), dehydrated with methanol, wash in 0.7×PBS, replaced in 15% and 30% sucrose, embedded in Frozen Section Compound Blue (Leica, Germany), and cut into 7-μm-thick sections. The sections were rehydrated in PBS for 5 min at room temperature, and then permeabilized and blocked in PBS containing 0.5% Triton X-100 and 5% bovine serum albumin for 1 hour at room temperature. They were then incubated with rabbit polyclonal anti-CYP17A1 (Mawaribuchi et al., 2014) and mouse monoclonal anti-VASA antibody (Komiya et al., 1994), diluted in PBS containing 2% skim milk (1:1000 and 1:500, respectively) overnight at 4°C. After washing with PBST (0.05% Triton X-100 in PBS) for 1 hour,

they were incubated with Alexa 546-conjugated goat anti-mouse IgG antibody and/or Alexa 488-conjugated goat anti-rabbit IgG antibody (Thermo Fisher Scientific, MA), diluted in PBS containing 2% skim milk (1:1000) for 1 hour at room temperature. After washing with PBST for 1 hour, they were mounted by 50% glycerol, and then observed by fluorescence microscopy (BZ-8000, Keyence; Osaka, Japan).

Sex steroid exposure

Estradiol was purchased from Wako (Osaka, Japan), and first dissolved in ethanol at 10 mM and then diluted with water. Tadpoles were grown in water at 300 nM of each sex steroid or 0.003% ethanol as a control at 22°C for 25 days.

Whole mount immunofluorescence

Samples were fixed with 4% paraformaldehyde in 0.7×PBS for 30 min at 4°C, and then permeabilized by 1% Triton X-100 in 0.7×PBS for 20 hours at 4°C. They were incubated in a blocking buffer containing 5% skim milk in 0.7×PBS with 0.05% Triton X-100 (0.7xPBS-T) for 3 hours at room temperature, and diluted the mouse monoclonal anti-VASA antibody (1:1000) and rabbit polyclonal anti-CYP17A1 antibody (1:1000) in the blocking buffer at 4°C overnight. Next, they were washed in 0.7×PBS-T for 1.5 hours, incubated with diluted Alexa 488-conjugated goat anti-rabbit IgG antibody (1:1000) and Alexa 594-conjugated goat anti-mouse IgG antibody (1:1000) in the blocking buffer for 1.5 hours, and washed in 0.7xPBS-T for 1.5 hours at room

temperature. They were then examined by fluorescence stereomicroscopy (MZ16F, Leica; Germany).

Statistical analysis

All values are expressed as the mean ±SEM. parametric statistical analysis was performed using the Student's t test. P values < 0.01 were considered statistically significant.

RESULTS

1. Expression analyses of several sex-related genes during ZZ and ZW gonadal development

In mammals, an *Sry*-type transcription factor gene *Sox9* and nuclear receptor genes *Sf1* (also known as *Ad4bp*) and *Dax1* are involved in *Sry*-driven sex determination and differentiation (Sekido and Lovell-Badge, 2008). Therefore I investigated whether *X. laevis* orthologs of these three genes might exhibit dimorphic expression between ZW and ZZ gonads after sex determination. In *X. laevis*, early gonadal differentiation starts after sex determination at stages 48-49. At stage 56, ZW and ZZ gonads exhibit distinct morphological differences: ZW gonads have ovarian cavities and primary oocytes, whereas germ stem cells migrate into medulla in the ZZ gonads (Yoshimoto et al., 2008). *X. laevis* has an allotetraploid genome consisting of L and S subgenomes (Session et al., 2016). Because there are two homoelogous L and S genes for *dax1, sf1,* and *sox9* in the genome, I employed common primers for each gene in quantitative RT-PCR. The analysis revealed that *dax1* and *sox9* showed approximately five to ten times higher expression in the ZZ than in the ZW gonads at stages 53 and 56 (Figs. 1A and 1C), indicating the involvement of early testicular formation. Expression of *dax1* mRNA was higher in ZZ testes after metamorphosis (Fig. 1A). In contrast, the expression of *sf1* mRNA in ZZ was two-folds than in ZW gonads throughout the development after stage 50, including stages 53 and 56 (Fig. 1B).

AMH, a member of TGF-β family, and its signaling is involved in sex (male) determination in two species of teleosts (Hattori et al., 2012; Kamiya et al., 2012).

Another member gene *inhbb* participates in early testicular development in mice (Yao et al., 2006). Therefore I examined whether these TGF-β family genes could display sexually dimorphic expression during gonadal development in *X. laevis*. Two homoelogous *amh* or *inhbb* genes exist in the species. Because I could not design a common primer pair for the *amh* or *inhbb* genes, I performed quantitative RT-PCR using a specific primer pair for each gene in the ZW and ZZ gonads at various stages after sex determination. *amh.L* cDNA could not be amplified. The analysis revealed that all of the three genes, *amh.S, inhbb.L* and *inhbb.S* showed greatly higher expression in ZZ than in ZW gonads throughout tadpole and frog development (Figs. 1D, 1E, and 1F). Notably, the expression of mRNAs of these genes was significantly higher in ZZ gonads at stage 50 immediately after sex determination, and then showed drastic increase at stage 53 followed by constantly high expression during testicular development.

2. Unique localization of *amh* and *inhbb* transcripts before and during deconstruction of the mass-in-line structure in developing testes

To understand the topological expression of *amh* and *inhbb* transcripts in developing testes during primary sex differentiation, I performed whole mount in situ hybridization (WISH) for these genes in ZW and ZZ gonads at stages 53 and 55. Both sex gonads at stage 53 shared the mass-in-line structure, which is required for ovarian differentiation, although it disappeared in ZZ gonads at stage 56 (Mawaribuchi et al., 2014). The 520 and 761 nucleotide sequences of the *amh.S* and *inhbb.S* probes shared

91% and 93% identities with corresponding sequences for *amh.L* and *inhbb.L*, respectively. Each antisense probe for *amh.S* or *inhbb.S* transcripts specifically reacted with ZZ gonads, but not with ZW gonads as shown in Fig. 2. Interestingly, staining patterns for *amh.S* or *inhbb.S* appeared to be similar at stage 53; both were expressed in cell masses on the mass-in-line structure. However, the patterns were somewhat different; *amh.S* and *inhbb.S* were expressed in the inner and outer sides of the masses, respectively (Fig. 2). At stage 55, the mass-in-line structure was under destruction, and the localization patterns of the two mRNAs in the stage were similar.

Next, I prepared transverse and sagittal sections of the stained gonads after the WISH analysis. To confirm the distinct expression patterns of the two genes, the sections were immunostained with a polyclonal antibody against *X. laevis* CYP17A1 (Mawaribuchi et al., 2014) and a monoclonal antibody against *Xenopus* VASA-like protein (Komiya *et al.,* 1994) in addition to the treatment with Hoechst 33258 for nuclear staining. In *X. laevis*, an androgen-synthesizing enzyme CYP17A1 is specifically localized in the masses of stage 53 gonads (Mawaribuchi et al., 2014), whereas the VASA-like protein shows specific expression in germ cells (Komiya *et al.,* 1994). I confirmed that *amh.S* and *inhbb.S* were expressed in the inner and outer sides of the masses consisting of CYP17-expressing cells, respectively, in both stage 53-sagital and -transverse sections (Figs. 3A and 3B). Although the mass-in-line structure was essentially destructed in stage 55 ZZ gonads as shown in the lower parts of Fig. 3A, expression patterns of the two genes were slightly similar to those at stage 53; most of the *amh.S* and *inhbb.S* transcripts appeared to remain in the center and

edges of the gonads, respectively, in both sagittal and transverse sections (Figs. 3A and 3B). I also observed that the two genes were not expressed in VASA-positive germ cells.

3. Maintenance of the mass-in-line structure by estrogen

Cell masses in the mass-in-line structure of ZW gonads consist of both CYP19A1- and CYP17A1-expressing cells that could produce estrogen, and those of ZZ gonads contain CYP17A1-expressing cells that could produce androgen (Mawaribuchi *et al.*, 2014). Because the mass-in-line structure disappeared at about stage 56 in ZZ gonads, it is possible that estrogen maintains the mass-in-line structure in ZW gonads. To verify this, I exposed ZW and ZZ tadpoles at stage 50 to estradiol for 25 days. Each gonad of the tadpoles, which developed at about stage 56, was used for whole mount immunofluorescence with the anti-CYP17A1 rabbit and anti-VASA mouse antibodies. My laboratory members previously reported that the expression of CYP17A1 was significantly lower in ZW than in ZZ gonads during tadpole development (Mawaribuchi et al., 2014). Predictably, a faint signal of CYP17A1 was detected in cell masses of both estrogen-treated and untreated (control) ZW gonads (Fig. 5). In contrast, CYP17A1 expression was positively detected in not only the control ZZ gonads, but also the estrogen-treated ZZ gonads. Importantly, the mass-in-line structure consisting of CYP17A1-positive cell masses was essentially maintained in the estrogen-treated ZZ gonads, although, in the control ZZ gonads, the CYP17A1 signal was spread out, indicating the destruction of the mass-in-line structure (Fig. 4B).

Interestingly, quantitative RT-PCR indicated that the expression levels of both *inhbb.L* and *inhbb.S* were significantly lower in the estrogen-treated ZZ gonads than in the control ZZ gonads (Fig. 6A and 6B). I also observed similar expression patterns of *amh.S* and *cyp17a1* (Fig. 6C and 6D).

At stage 53 and later, germ cells remained around the cell masses in ZW gonads. However, in ZZ gonads, they migrated from the cortex to the medulla and this migration was accompanied by the destruction of the mass-in-line structure (Mawaribuchi et al., 2014). In the control and estrogen-treated ZW gonads, there were many VASA-positive germ cells, which might remain at the outside of the cell masses (Fig. 5). Interestingly, VASA-positive germ cells migrated into the CYP17A1-expressing cell masses in not only the control ZZ gonads, but also the estrogen-treated ZW gonads, which retained the mass-in-line structure similar to ZW gonads (Fig. 5). Thus the estrogen-treated ZW gonads appeared to show ovotestes.

DISCUSSION

In amphibians, it remains unclear how gonadal sex differentiation following sex determination is molecularly controlled. In my laboratory, sexually dimorphic expression of mRNAs for *foxl2* and several steroidogenic genes or of proteins for DMRT1 and H2AXγ in developing gonads in *X. laevis* were previously reported (Okada et al., 2009; Mawaribuchi et al., 2014; Fujitani et al., 2016). In this study, I focused on *X. laevis* orthologs of mammalian sex-related genes *sf1, dax1, sox9, amh,* and *inhbb,* and examined whether their mRNA levels show dimorphic expressions between developing ZW and ZZ gonads. Quantitative RT-PCR analysis revealed higher mRNA levels of the nuclear receptor and/or transcription factor genes *dax1*, *sf1*, and *sox9* in ZZ male than in ZW female gonads during early gonadal differentiation (Figs. 1A, 1B, and 1C). In mouse fetal gonads, *dax1* and *sf1* mRNAs are expressed in somatic cells of both sexes, and the expression of *dax1* is higher in XX female than in XY male gonads (Ikeda *et al*., 2001). Sugita *et al*. (2001) reported that the frog *Rana rugosa* DAX1 might play a role in testicular development, because *dax1* transcription is involved in female-to-male sex reversal upon the administration of testosterone. In the teleost fish medaka, *dax1* mRNA is not detected in both female and male gonads during early sex differentiation, although DAX1 might suppress SF1-driven transcription of aromatase *cyp19a1* gene in adult ovarian follicles (Nakamoto *et al*., 2007). These findings suggest that DAX1 function in gonadal formation and differentiation has diverged during vertebrate evolution. However, functional repression of SF1 by DAX1 might be

conserved among vertebrates.

In eutherian mammals, SRY together with SF1 could directly up-regulate the transcription of *Sox9* via its cis-regulatory element named TESCO (testis-specific enhancer of SOX9 core element), and the resultant SOX9 could lead to testicular differentiation (Sekido and Lovell-Badge, 2008). In reptilians and birds, *sox9* is expressed at a higher level in developing testes vs. developing ovaries (Rhen and Schroeder, 2010; Cutting et al., 2013). Intriguingly, in medaka, *sox9* plays a role in germ cell maintenance, and is not required for testis determination; the functionless mutants of *sox9* exhibit female-to-male sex reversal (Nakamura et al., 2012). In the present study, *sox9* mRNA showed higher expression in ZZ than in ZW gonads during tadpole development after sex determination, suggesting that *sox9* plays a role in early testicular differentiation in *X. laevis* (Figs. 1C and 7). It will be interesting to clarify the functions of SOX9 in gonadal somatic cells during vertebrate evolution.

TGF-β family members are involved in male sex determination and testicular differentiation in various vertebrates (Itman *et al.,* 2006; Barakat *et al*., 2012; Hattori *et al*., 2012; Kamiya *et al*., 2012; Myosho *et al*. 2012; Cutting et al., 2013; Ito and Mawaribuchi, 2013; Kodama et al., 2015). However, the role of TGF-β family members in gonadal formation in *X. laevis* is not fully understood. In this study, two types of genes encoding members of this family, *amh.S and inhbb.L/S*, showed substantially higher expression in ZZ than in ZW gonads during primary gonadal differentiation immediately after sex determination in this species (Fig. 1D, 1E, and 1F). Patagonian pejerrey Y-linked *amh* (*amhy*) and *Takifugu rubripes* Y-linked AMH receptor gene

amhr2 are involved in testis formation and act as sex determinants (Hattori *et al*., 2012; Kamiya *et al*., 2012). High expression of *amh* occurs in an early stage of testis formation before the onset of *Sox9* expression in chicken (Takada *et al*., 2005). In contrast, in mammals, AMH secreted from Sertoli cells functions as an anti-Müllerian hormone (Vigier et al., 1985), but it does not appear to function as a testis-forming factor. Therefore it is possible that AMH has a conserved role for primary testicular development in non-mammalian vertebrates. In addition to quantitative RT-PCR analysis, I performed in situ hybridization of developing ZW and ZZ gonads using *amh.S* or *inhbb.S* probes. Because sequence identity in the probes between *amh.S* and *amh.L or inhbb.S* and *inhbb.L* was substantially high (91% or 93%, respectively), the signals might be derived not only form *amh.S*/*inhbb.S,* but also *amh.L*/*inhbb.L.* Anyway, the *amh* and *inhbb* mRNAs are localized differently in cell masses of the mass-in-line structure (Figs. 2 and 3), suggesting that AMH and inhibin signals might play distinct roles in early testicular formation. As *inhbb* mRNA was detected in the outer sides of the cell masses, I hypothesized that a homodimer of INHBB, Activin B acts as ligands for the destruction of the mass-in-line structure, leading to the formation of testicular structures. In mice, *inhbb* contributes to the formation of testis-specific vasculature after sex determination (Yao et al., 2006). These findings suggest that the product of *inhbb* might have a conserved role in the construction of primary testis-specific structures as an intercellular masculinization ligand. However that may be, it is necessary to identify cells that express each receptor and to clarify intracellular signaling mediated through Smads in the cells, and to produce and analyze crispr/cas9-driven knockout tadpoles and

frogs for *amh* or *inhbb* for understanding the distinct functions of inhibin and AMH signaling in testis formation.

The destruction of the mass-in-line structure in ZZ gonads might be induced by androgens and cytokines such as inhibins (Figs. 2 and 3). Conversely, there must be factors for the maintenance of the mass-in-line structure in the undifferentiated ZW gonads. Estrogen could induce feminization in bipotential gonads in various non-mammalian vertebrates. In fact, exposure to estrogen before and during sex determination can cause male-to-female sex reversal (Villalpando et al., 1990), and estrogen-synthesizing gene *cyp19a1* displays predominant expression in cell masses of ZW gonads immediately after sex determination (Mawaribuchi et al., 2014). Predictably, estrogen prevented the disappearance of the mass-in-line structure in ZZ gonads (Fig. 5). Collectively, we propose a model for early gonadal differentiation after sex determination from a viewpoint of the relationships among gene expression cascade, sex-specific ligands, and development of the mass-in-line structure (Fig. 7). In ZW gonads, DM-W induces up-regulation of the estrogen-synthesizing enzyme gene *cyp19a1* and the feminizing gene *foxl2*. Then estrogens maintain the mass-in-line structure after sex determination as a ligand for feminization. In ZZ gonads, *dax1*, *sox9*, *sf1*, *inhbb* and *amh* are highly upregulated after sex determination because of the absence of DM-W. A homodimer of INHBB, Activin B, induces the deconstruction of the mass-in-line structure as a ligand for masculinization.

Very interestingly, germ cells migrated into cell masses in the estrogen-treated ZZ gonads as in the control ZZ gonads, although they retained around

the cell masses in both the estrogen-treated and untreated ZW gonads. These findings suggest that estrogen, which is produced by the *cyp19a1*-expressing cell masses, can function to maintain the mass-in-line (cell-mass) structure in ZW gonads, although it may not directly participate in blocking germ cell migration into cell masses. In the future, it will be interesting to clarify the relationships between the mass-in-line structure and sex steroids in other amphibian species such as the Japanese frog *Glandirana rugosa*, which has regional changes in sensitivity to sex steroid-induced sex reversal (Miura et al., 2016). It will also be intriguing to unveil the crosstalk between TGF-β and estrogen signalings.

ACKNOWLEDGEMENTS

I am grateful to Prof. Nobuhiko Takamatsu for his continuous encouragement and support. I am also grateful to Assoc. Prof. Michihiko Ito for his support, encouragement and many helpful discussions for this study, to Dr. Kei Tamura, Dr. Shuji Mawaribuchi and Ms Kazuko Fujitani for many helpful discussions and advices.

Finally, I would like to express sincere thanks to my family for their supports.

REFERENCES

Barakat B, Itman C, Mendis SH, Loveland KL (2012) Activins and inhibins in mammalian testis development: new models, new insights. Mol Cell Endocrinol 359: 66-77

Cutting A, Chue J, Smith CA (2013) Just how conserved is vertebrate sex determination? Dev Dyn 242: 380-38

Fujitani K, Otomo A, Wada M, Takamatsu N, Ito M (2016) Sexually dimorphic expression of Dmrt1 and γH2AX in germ stem cells during gonadal development in *Xenopus laevis*. FEBS Open Bio 6: 276-284

Ikeda Y, Takeda Y, Shikayama T, Mukai T, Hisano S, Morohashi KI (2001) Comparative localization of Dax-1 and Ad4BP/SF-1 during development of the hypothalamic-pituitary-gonadal axis suggests their closely related and distinct functions. Dev Dyn 220: 363-376

Kamiya T, Kai W, Tasumi S, Oka A, Matsunaga T, Mizuno N, Fujita M, Suetake H, Suzuki S, Hosoya S, Tohari S, Brenner S, Miyadai T, Venkatesh B, Suzuki Y, Kikuchi K (2012) A trans-species missense SNP in Amhr2 is associated with sex determination in the tiger pufferfish, Takifugu rubripes (fugu). PLoS Genet 8: e1002798

Komiya T, Itoh K, Ikenishi K, Furusawa MA (1994) Isolation and characterization of a novel gene of the DEAD box protein family which is specifically expressed in germ cells of *Xenopus laevis*. Dev Biol 162: 354-363

Hattori RS, Murai Y, Oura M, Masuda S, Majhi SK, Sakamoto T, Fernandino JI, Somoza GM, Yokota M, Strüssmann CA (2012) A Y-linked anti-Müllerian hormone duplication takes over a critical role in sex determination. Proc Natl Acad Sci U S A 109: 2955-2959

Itman C, Mendis S, Barakat B, Loveland KL (2006) All in the family: TGF-beta family action in testis development. Reproduction. 132: 233-246

Kodama M, Suda M, Sakamoto D, Iwasaki T, Matsuo Y, Uno Y, Matsuda Y, Nakamura Y, Maekawa S, Katsu Y, Nakamura M (2015) Molecular cloning and characterization of anti-Müllerian hormone (AMH) from the Japanese wrinkled frog, Rana rugosa. Endocrinology 156: 1914-1923.

Mawaribuchi S, Ikeda N, Fujitani K, Ito Y, Onuma Y, Komiya T, Takamatsu N, Ito M (2014) Cell-mass structures expressing the aromatase gene Cyp19a1 lead to ovarian cavities in *Xenopus laevis*. Endocrinology 155: 3996-4005

Mawaribuchi S, Ito M (2013) Molecular Evolution of Genes Involved in Vertebrate Sex Determination. In: eLS. John Wiley & Sons Ltd, Chichester.

Miura I, Ohtani H, Ogata M, Ezaz (2016) Evolutionary Changes in Sensitivity to Hormonally Induced Gonadal Sex Reversal in a Frog Species. Sex Dev 10: 79-90

Myosho T, Otake H, Masuyama H, Matsuda M, Kuroki Y, Fujiyama A, Naruse K, Hamaguchi S, Sakaizumi M (2012) Tracing the emergence of a novel sex-determining gene in medaka, Oryzias luzonensis. Genetics 191: 163-170

Nakamoto M, Wang DS, Suzuki A, Matsuda M, Nagahama Y, Shibata N (2007) Dax1 suppresses P450arom expression in medaka ovarian follicles. Mol Reprod Dev 74: 1239-1246

Nakamura S, Watakabe I, Nishimura T, Toyoda A, Taniguchi Y, Tanaka M (2012) Analysis of medaka sox9 orthologue reveals a conserved role in germ cell maintenance. PLoS One 7: e29982

Okada E, Yoshimoto S, Ikeda N, Kanda H, Tamura K, Shiba T, Takamatsu N, Ito M (2009) *Xenopus* W-linked DM-W induces Foxl2 and Cyp19 expression during ovary formation. Sex Dev 3: 38-42

Mawaribuchi S, Ikeda N, Fujitani K, Ito Y, Onuma Y, Komiya T, Takamatsu N, Ito M (2014) Cell-mass structures expressing the aromatase gene Cyp19a1 lead to ovarian cavities in *Xenopus laevis*. Endocrinology 155: 3996-4005

Rhen T, Schroeder A (2010) Molecular mechanisms of sex determination in reptiles. Sex Dev 4: 16-28

Sekido R, Lovell-Badge R (2008) Sex determination involves synergistic action of SRY and SF1 on a specific Sox9 enhancer. Nature 453: 930-934

Session AM et al (2016) Genome evolution in the allotetraploid frog *Xenopus laevis*. Nature 538: 336-343

Sugita J, Takase M, Nakamura M (2001) Expression of Dax-1 during gonadal development of the frog. Gene 280: 67-74

Vigier B, Picard JY, Campargue J, Forest MG, Heyman Y, Josso N (1985) Secretion of anti-Müllerian hormone by immature bovine Sertoli cells in primary culture,

studied by a competition-type radioimmunoassay: lack of modulation by either FSH or testosterone. Mol Cell Endocrinol 43:141-150

Villalpando I, Merchant-Larios H (1990) Determinationo of the sensitive stages for gonadal sex-reversal in *Xenopus laevis* tadpoles. Int J Dev Biol 34: 281–285

Yao HH, Aardeme J, Holthusen K (2006) Sexually dimorphic regulation of inhibin beta B in establishing gonadal vasculature in mice. Biol Reprod 74: 978-983

Yoshimoto S, Ito M (2011) A ZZ/ZW-type sex determination in *Xenopus laevis*. FEBS J. 278: 1020-1026.

Yoshimoto S, Okada E, Umemoto H, Tamura K, Uno Y, Nishida-Umehara C, Matsuda Y, Takamatsu N, Shiba T, Ito M (2008) A W-linked DM-domain gene, DM-W, participates in primary ovary development in *Xenopus laevis*. Proc Natl Acad Sci U S A 105: 2469-2474

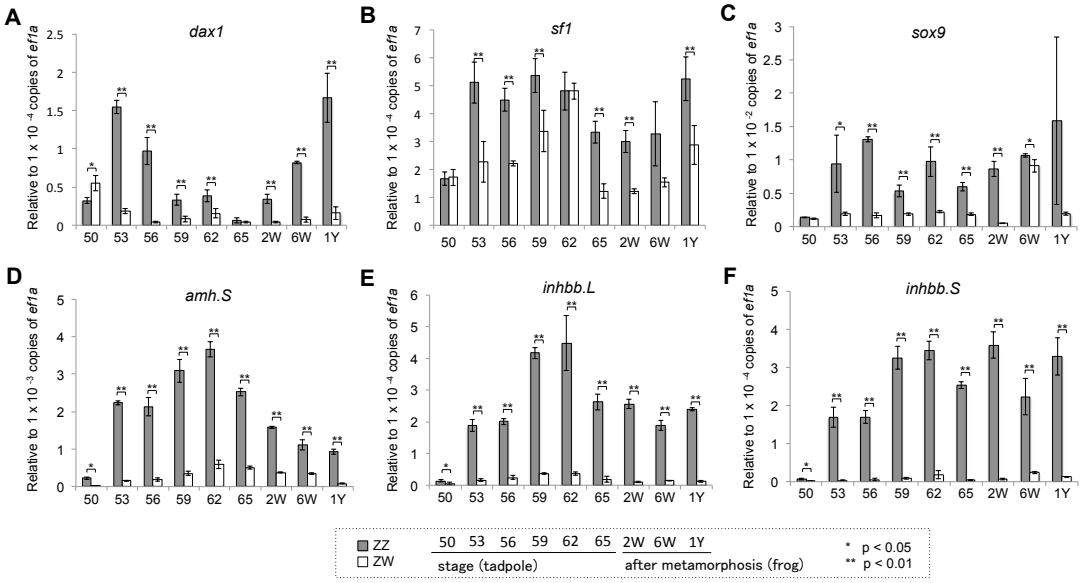

Fig. 1. Real-time RT-PCR analysis of *dax1*, *sf1*, *sox9,* and TGF-β family genes, *amh* and *inhbb* in ZZ and ZW gonads during sexual development in *X. laevis*. qPCR was performed for *dax1* (A), *sf1* (B), *sox9* (C), *amh.S* (D), *inhbb.L* (E), and *inhbb.S* (F) using cDNAs derived from the total RNAs of ZZ and ZW gonads from tadpoles at different developmental stages (50-65) and adult frogs at two weeks (2W), six weeks (6W), and one year (1Y) after metamorphosis. Common sequences between *dax1.L and S*, *sf1.L* and *S,* or *sox9.L* and *S* cDNAs were used as each primer pair. *ef-1a* was used for normalization. Values are the mean ± s.d. of three individual experiments. *: $p < 0.05$; **: $p < 0.01$ by two-tailed student's t-test. Horizontal axis represents developmental stages and time (W, weeks; Y, year) after metamorphosis.

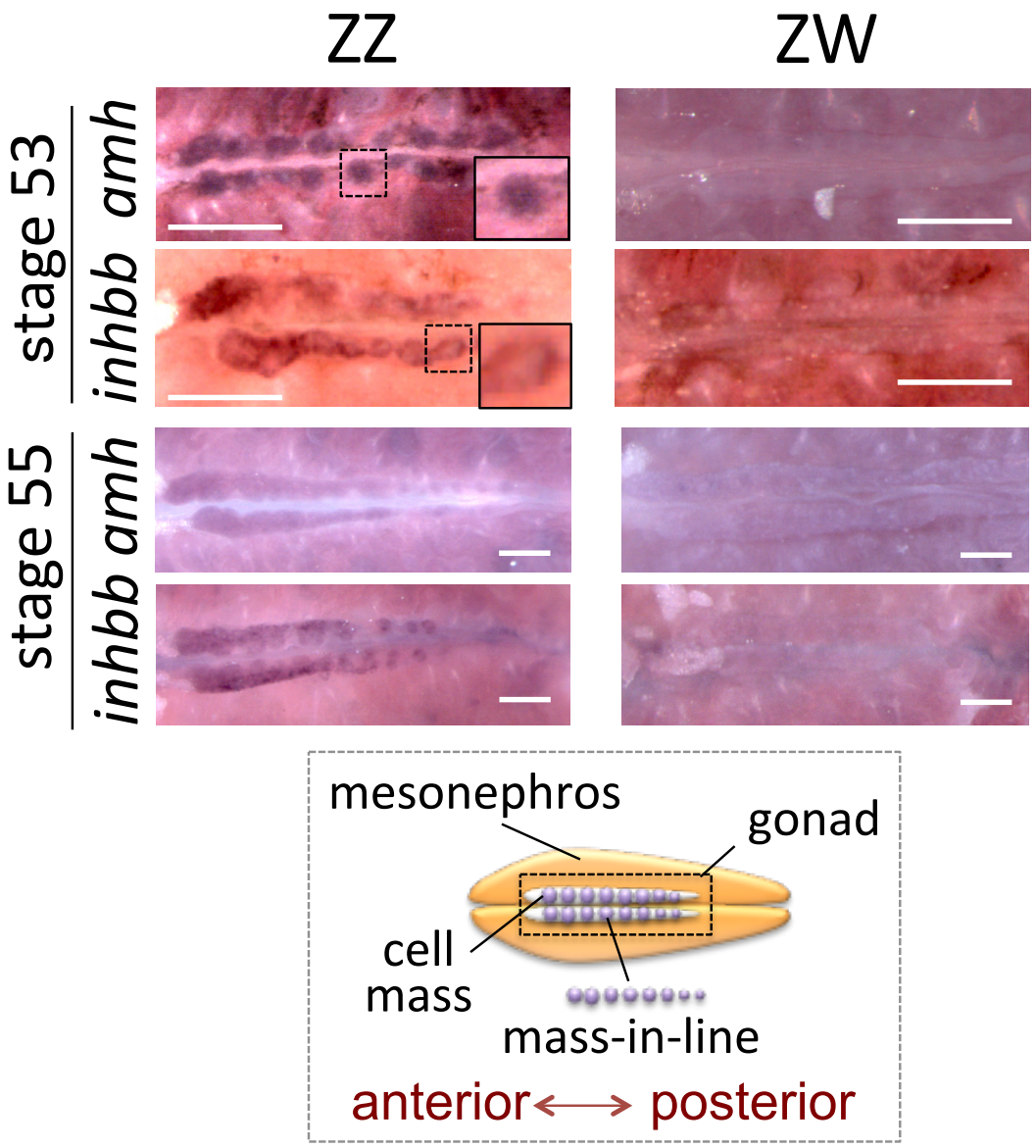

Fig. 2. Whole mount in situ hybridization (WISH) analysis for *amh* and *inhbb* transcripts in developing ZZ and ZW gonads. WISH of ZZ and ZW gonads with the mesonephros at stages 53 and 55 was performed using the antisense RNA probe for *amh.S* or *inhbb.S* mRNA. Gonads are lying on the mesonephros in ventral view. "cell mass" and "mass-in-line" are pointed in its schematic drawing. Scale bars, 200 μm.

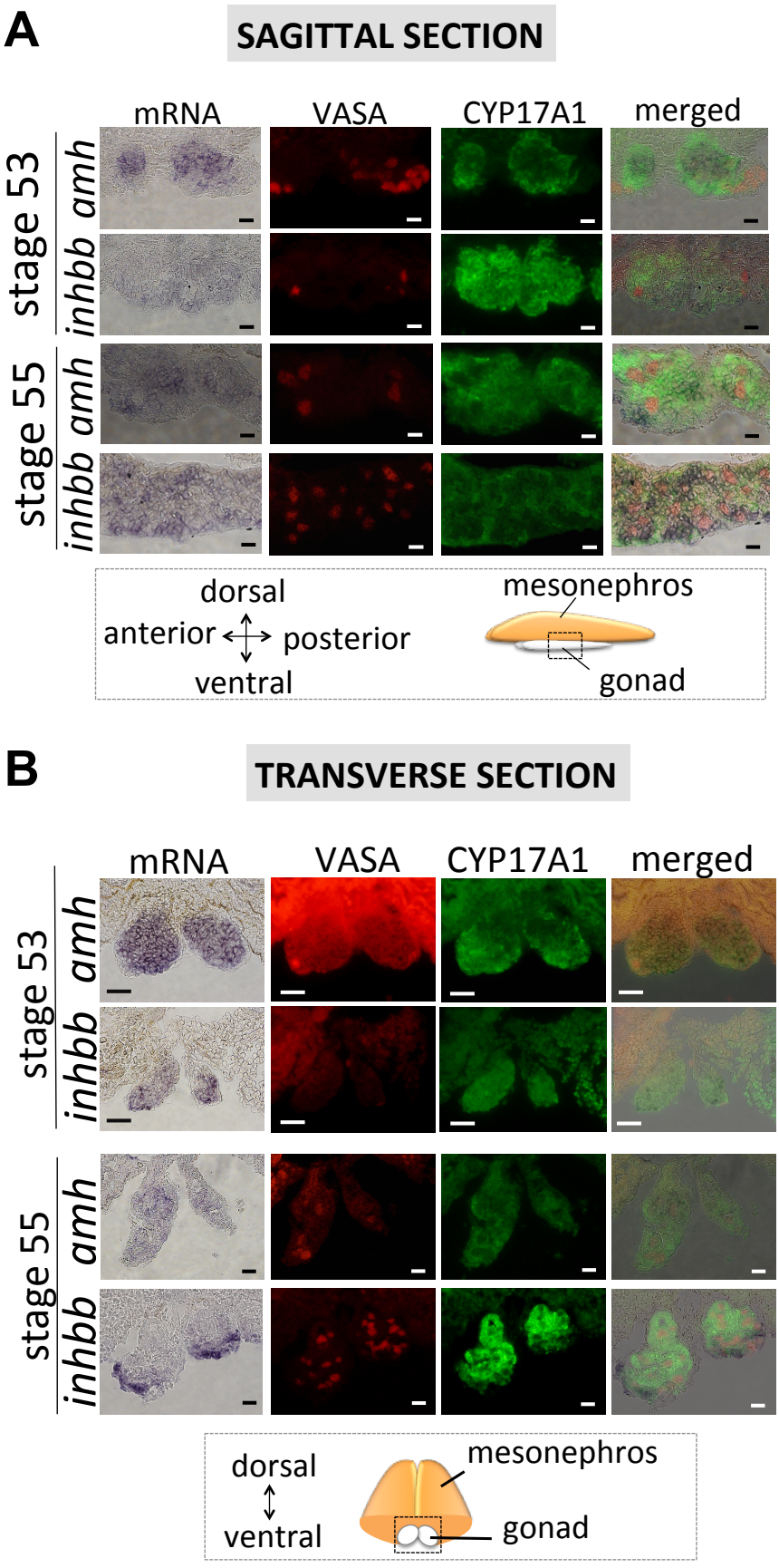
A
SAGITTAL SECTION
mRNA
VASA
CYP17A1
merged
stage 53
amh
inhbb
stage 55
amh
inhbb
dorsal
anterior
posterior
ventral
mesonephros
gonad
B
TRANSVERSE SECTION
mRNA
VASA
CYP17A1
merged
stage 53
amh
inhbb
stage 55
amh
inhbb
dorsal
ventral
mesonephros
gonad

Fig. 3. Immunohistochemical analysis on the sections of developing ZZ gonads after the WISH analysis for *amh* and *inhbb* mRNAs. The ZZ gonads at stages 53 and 55 after the WISH analysis were sectioned sagittally (A) or transversely (B) at 7 μm using a cryostat. The sections were treated with an anti-CYP17A1 antibody (green) for the cell masses consisting of steroidogenic cells on the mass-in-line structure, and an anti-VASA antibody (red) for germ cells. Scale bars, 20 μm.

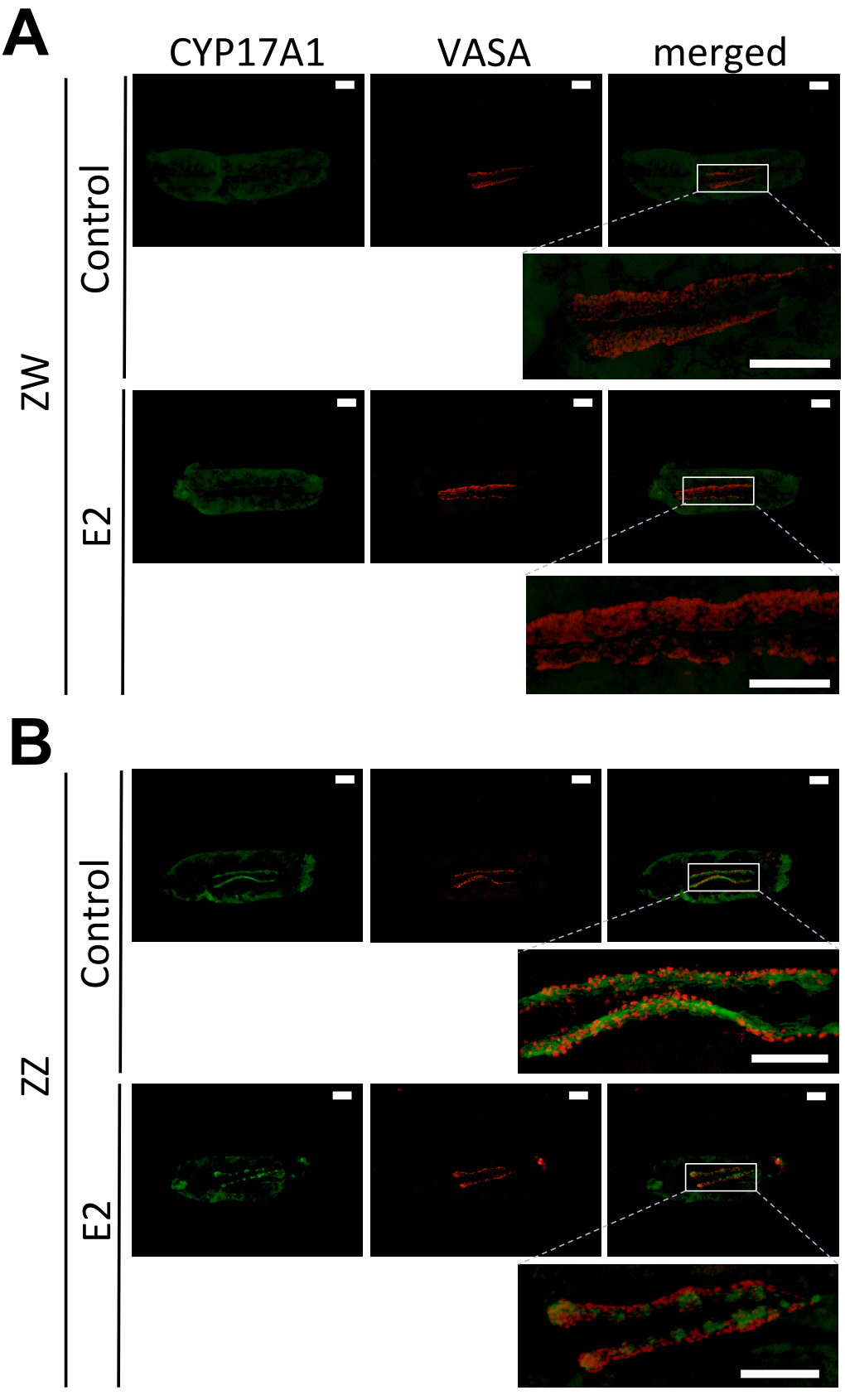
A
CYP17A1
VASA
merged
ZW
Control
E2
B
ZZ
Control
E2

Fig. 4. An effect of estrogen on the mass-in-line structure of developing ZZ or ZW gonads after sex determination.

Tadpoles at stage 50 just after sex determination were grown in the presence or absence (control: 0.003% ethanol vehicle) of 300 nM estradiol (one of estrogens) for 25 days. Whole mount immunofluorescence with anti-CYP17A1 (green) and anti-VASA (red) antibodies was performed for the gonads of estrogen-treated and non-treated (control) ZZ and ZW tadpoles at about stage 56. Gonads are lying on the mesonephros in ventral view. Anterior-posterior corresponds to left-right. Scale bars, 500 μm.

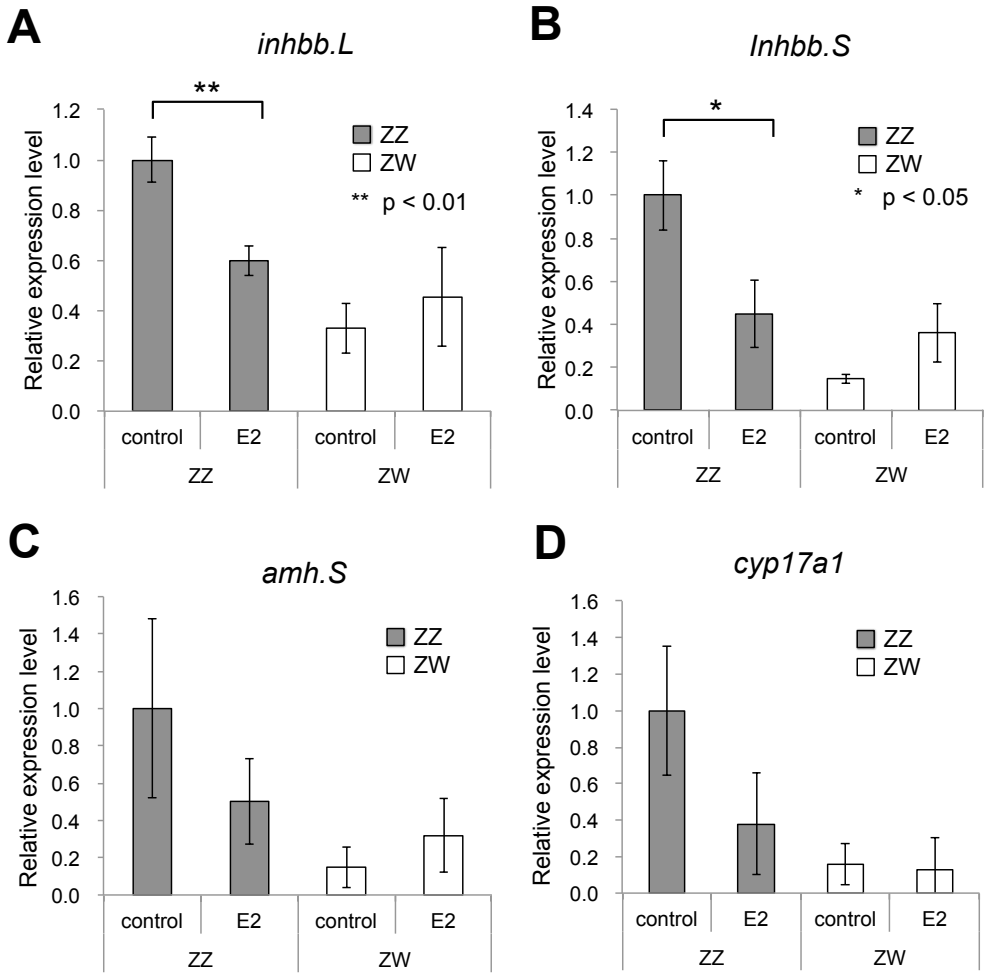

Fig. 5. Real-time RT-PCR analysis of *amh*, *inhbb*, and *cyp17a1* in estrogen-treated or untreated ZZ and ZW gonads.

The RT-PCR was performed for *inhbb.L* (A), *inhbb.S*, (B), *amh.S* (C), and *cyp17a1* (D) using cDNAs derived from the total RNAs of the gonads in estrogen-treated or untreated ZZ and ZW tadpoles at about stage 56, which were grown by the same method as in Fig. 5. *ef-1a* was used for normalization. Values are the mean ± s.d. of three individual experiments. *: $p < 0.05$; **: $p < 0.01$ by two-tailed student's t-test.

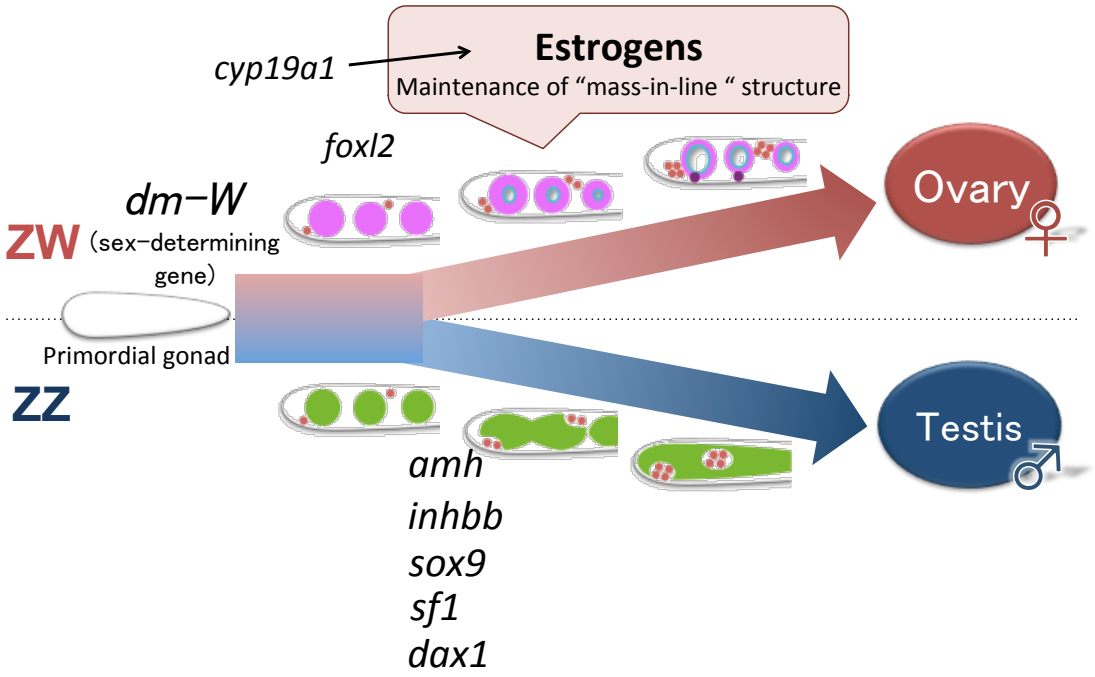

Fig. 6. Proposed model for early ovary or testis formation based on the mass-in-line structure in *X. laevis*.

In undifferentiated ZW gonads during sex determination, DM-W induces up-regulation of *cyp19a1* encoding the estrogen-synthesizing enzyme aromatase and the feminizing gene *foxl2*. Estrogens maintain the mass-in-line structure, which leads to ovarian cavity formation in differentiating ZZ gonads after sex determination. In contrast, in the absent of DM-W, transcription levels of *dax1*, *sox9*, *sf1*, *inhbb* and *amh* are up-regulated in differentiating ZZ gonads.